

## ***Supporting information***

### **An Aza-BODIPY based NIR-II luminogen enables efficient phototheranostics**

Na Yang<sup>ab</sup>, Shuang Song<sup>b</sup>, Chang Liu<sup>ab</sup>, Jia Ren<sup>ab</sup>, Xin Wang<sup>cd</sup>, Shoujun Zhu<sup>cd</sup> and  
Cong Yu<sup>\*ab</sup>

a School of Applied Chemistry and Engineering, University of Science and Technology of China,  
Hefei 230026, P.R. China.

b State Key Laboratory of Electroanalytical Chemistry, Changchun Institute of Applied Chemistry,  
Chinese Academy of Sciences, Changchun 130022, P.R. China.

c Joint Laboratory of Opto-Functional Theranostics in Medicine and Chemistry, The First  
Hospital of Jilin University, Changchun 130021, P.R. China.

d State Key Laboratory of Supramolecular Structure and Materials, College of Chemistry, Jilin  
University, Changchun 130012, P.R. China.

## **Experimental section**

### **Materials**

All chemical reagents were purchased from Aladdin or Energy Chemical Co., Ltd. Commercially available reagents were analytical reagent grade and used directly without further purification. Fetal bovine serum (FBS), RPMI 1640 medium and trypsin-EDTA were purchased from Gibco Life Technologies. CellTiter 96® Aqueous One Solution Cell Proliferation Assay Kit (MTS) was purchased from Promega Biotech Co., Ltd. Rat 4T1 and L929 cell lines were obtained from Shanghai Institute of Biochemistry and Cell Biology, Chinese Academy of Sciences. Millipore

deionized (DI) water ( $18.2 \text{ M}\Omega \text{ cm}^{-1}$ ,  $25 \text{ }^\circ\text{C}$ ) was used to prepare all assay solutions.

### **Characterization**

$^1\text{H}$  and  $^{13}\text{C}$  NMR spectra were recorded on a Bruker Avance III 500/400 MHz spectrometer using residual proton or carbon signal of the deuterated solvent as internal standard. Mass spectra were recorded on a Bruker Mass spectrometer (Bruker Daltonics flex analysis). Chemical shifts are reported in parts per million. H-600 electron microscope (TEM, Hitachi, Japan) was used to characterize the morphology of the CB1 nanoparticles. Cary 50 Bio Spectrophotometer (Varian Inc., CA, USA) was used to record the UV–vis absorption spectra using a 1 cm cuvette. Fluorescence emission spectra were recorded using a FluoroLog-3 spectrofluorometer (Horiba Inc., USA) at an ambient temperature. Confocal laser scanning microscope (CLSM) images were obtained using a Nikon ECLIPSE Ti microscope (Japan). Cell viability data were recorded by a Synergy microplate reader (BioTek, USA).

### **Synthesis of B-1**

1.77 g diethylaminobenzaldehyde and 1.99 g 4-bromoacetophenone were mixed in 20 mL EtOH, and then NaOH solution (2.5 M, 10 mL) was added. The reaction solution was stirred at room temperature for 24 h, a yellow solid was filtered and dried without further purification.  $^1\text{H}$  NMR (400 MHz,  $\text{DMSO-}d_6$ )  $\delta$  (ppm): 8.04 (d,  $J = 8.5 \text{ Hz}$ , 2H), 7.75 (d,  $J = 8.5 \text{ Hz}$ , 2H), 7.71-7.58 (m, 4H), 6.71 (d,  $J = 8.9 \text{ Hz}$ , 2H), 3.42 (q,  $J = 7.0 \text{ Hz}$ , 4H), 1.13 (t,  $J = 7.0 \text{ Hz}$ , 6H).

### Synthesis of B-2

1 g compound B-1 was dissolved in a mixture of methanol (10 mL), diethylamine (7.5 mL) and nitromethane (4 mL), and the reaction mixture was refluxed overnight. After cooling to room temperature, 1 M HCl was used to neutralize the solution, and the crude product was extracted with CH<sub>2</sub>Cl<sub>2</sub> (3×50 mL). Na<sub>2</sub>SO<sub>4</sub> was used to dry the combined organics. Solvent was cleaned up under reduced pressure. The final product was acquired by chromatography (petroleum ether/EtOAc, 4:1). <sup>1</sup>H NMR (400 MHz, CDCl<sub>3</sub>) δ (ppm): 7.77 (d, *J* = 8.5 Hz, 2H), 7.59 (d, *J* = 8.5 Hz, 2H), 7.07 (d, *J* = 8.6 Hz, 2H), 6.59 (d, *J* = 8.6 Hz, 2H), 4.77-4.72 (m, 1H), 4.65-4.60 (m, 1H), 4.09-4.05 (m, 1H), 3.38-3.28 (m, 6H), 1.13 (t, *J* = 7.0 Hz, 6H).

### Synthesis of C-1

0.35 g B-2 and 0.35 g 4-(diphenylamino)phenylboronic acid were dissolved in a solution of toluene/EtOH (5:1, 25 mL). Nitrogen was bubbled through the solution for 10 min, 57 mg Pd(PPh<sub>3</sub>)<sub>4</sub> and Na<sub>2</sub>CO<sub>3</sub> (2 eq of 1 M aqueous solution) were added, and the reaction mixture was stirred under nitrogen at reflux for 16 h. The reaction mixture was cooled, filtered, and EtOAc/water 1:1 (50 mL) was added. The organic layer was separated, and the aqueous layer was extracted with EtOAc (2 × 25 mL). The combined organics were dried over MgSO<sub>4</sub>, and solvent was evaporated under reduced pressure. The crude product was purified by column chromatography (CH<sub>2</sub>Cl<sub>2</sub> to CH<sub>2</sub>Cl<sub>2</sub>/EtOAc 3:1). <sup>1</sup>H NMR (500 MHz, CDCl<sub>3</sub>) δ (ppm): 7.97-7.94 (m,

2H), 7.65-7.61 (m, 2H), 7.49 (m, 2H), 7.31-7.24 (m, 4H), 7.16-7.03 (m, 10H), 6.60 (d,  $J = 8.2$  Hz, 2H), 4.80-4.77 (m, 1H), 4.66-4.62 (m, 1H), 4.13-4.10 (m, 1H), 3.43-3.39 (m, 2H), 3.31 (q,  $J = 7.0$  Hz, 4H), 1.13 (t,  $J = 7.0$  Hz, 6H).

### Synthesis of C-2

0.58 g compound C-1 and 1.50 g ammonium acetate were mixed in 10 mL n-butanol, then reacted at 100 °C for 24 h. After solvent was removed, the residue was filtered and washed with cool ethanol three times. Compound C-2 of blue color was used directly without further purification.

### Synthesis of CB1

0.11 g compound C-2 was dissolved in a mixture of dry  $\text{CH}_2\text{Cl}_2$  (0.25 mL), DIEA (0.7 mL) and  $\text{BF}_3 \cdot \text{OEt}_2$  (0.39 mL, 3.12 mmol). The solution was reacted at room temperature for 12 h. The final product CB1 as blue solid was acquired by chromatography ( $\text{CH}_2\text{Cl}_2$ /hexane, 3:2).  $^1\text{H}$  NMR (500 MHz,  $\text{CDCl}_3$ )  $\delta$  (ppm): 8.14-8.09 (m, 8H), 7.67-7.66 (m, 4H), 7.54-7.53 (m, 4H), 7.30-7.26 (m, 10H), 7.16-7.12 (m, 10H), 7.06-7.03 (m, 4H), 6.88 (s, 2H), 6.76-6.74 (m, 4H), 3.48-3.46 (q,  $J = 7.2$  Hz, 8H), 1.26 (t,  $J = 7.2$  Hz, 12H);  $^{13}\text{C}$  NMR (101 MHz,  $\text{CDCl}_3$ ) (ppm): 156.79, 148.57, 147.63, 143.34, 142.03, 131.32, 129.94, 129.36, 127.83, 126.49, 125.12, 124.69, 123.67, 123.53, 123.16, 114.77, 111.44, 44.70, 29.75, 12.79; MALDI-MS: calculated for  $\text{C}_{76}\text{H}_{66}\text{BF}_2\text{N}_7$   $[\text{M}]^+$  1125.54, found 1125.6.

### **Preparation of the CB1 nanoparticles**

THF solution (1 mL) containing DSPE-mPEG2000 (3 mg) and CB1 (0.2 mg) were added dropwise into an aqueous solution (10 mL), and the mixture was stirred for 8 h at ambient temperature to evaporate the organic solvent. Purified CB1 NPs were obtained by ultrafiltration.

### **Fluorescence quantum yield measurement**

ICG (QY = 13% in DMSO, Ex = 808 nm) was used as reference fluorophore to calculate the quantum yield of CB1 and the CB1 NPs. The quantum yield was calculated as follows:<sup>S1</sup>

$$\Phi = \Phi_{ref} \times (n^2_{sample}/n^2_{ref}) (I_{sample}/A_{sample}) (A_{ref}/I_{ref})$$

UV-vis absorbance values of CB1 or the CB1 NPs at difference concentrations were measured, and the integrated fluorescence intensity was plotted against the absorbance value. Comparison of the slope led to the quantum yield of the fluorophore.

### **Photothermal conversion efficiency of the CB1 and CB1 NPs**

CB1 NPs in water was irradiated by laser (808 nm, 1 W cm<sup>-2</sup>) for 10 min and then cooled to room temperature. The temperature changes were recorded by a temperature probe. Photothermal conversion efficiency was calculated according to the following equations (1-5).<sup>S2</sup>

$$\eta = \quad (1)$$

$$\frac{hS(T_{max} - T_{amb}) - Q_{Dis}}{I(1 - 10^{-A_{808}})}$$

$$\theta = \frac{T - T_{amb}}{T_{max} - T_{amb}} \quad (2)$$

$$dt = -\tau S \frac{d\theta}{\theta} \quad (3)$$

$$\tau S = \frac{\sum_i m_i C_{p,i}}{hS} \quad (4)$$

$$t = -\tau S \ln(\theta) \quad (5)$$

where  $h$  is the heat transfer coefficient,  $S$  is the surface area of the container.  $T_{max}$  is the maximum steady-state temperature of the CB1 NPs containing aqueous solution,  $I$  is the laser power density,  $A_{808}$  is the absorbance of the CB1 NPs at 808 nm and  $Q_{Dis}$  is the heat associated with light absorption by the solvent. The variable  $\tau S$  is the sample-system time constant, and  $m_i$  and  $C_i$  are the mass and heat capacity ( $4.2 \times 10^3$  J/kg °C) of deionized water.

CB1 in aqueous solution (1% DMSO in water) was irradiated by laser (808 nm, 1 W cm<sup>-2</sup>) for 10 min and then cooled to room temperature. The temperature changes were recorded by a temperature probe. Photothermal conversion efficiency was calculated.

### Cell culture

4T1 and L929 cells were cultured in RPMI-1640 culture medium containing 10% fetal bovine serum and 1% antibiotics penicillin/streptomycin (100 U/mL) at 37 °C, 5% CO<sub>2</sub>.

## **Cytotoxicity**

Cytotoxicity of the CB1 NPs was evaluated by the traditional MTS assay.  $3 \times 10^4$  cells were seeded in a 96-well plate and grown overnight in an incubator. Various amounts of CB1 NPs were added and the samples were incubated for an additional 24 h. The culture medium was removed and 200  $\mu$ L of fresh culture medium was added. One set of the cell samples was irradiated with light for 10 min (808 nm). Another set was not irradiated. Then, the culture medium was removed and 100  $\mu$ L of fresh culture medium (containing 1% MTS) was added. The cells were further incubated for 3 h, and the absorption values at 490 nm were recorded by a microplate reader.

Cytotoxicity of CB1 was evaluated.  $3 \times 10^4$  cells were seeded in a 96-well plate and grown overnight in an incubator. CB1 was dissolved in DMSO as stock solution. The cell culture media with various amounts of CB1 (1% DMSO in RPMI-1640 culture medium) were added and further incubated for an additional 24 h, and the absorption values were recorded.

## **Live/dead co-staining assay**

$1 \times 10^5$  cells were seeded in a 6-well plate overnight and divided into four groups (control, control + laser, CB1, and CB1 + laser). For the CB1 NPs containing two groups, cells were treated with the CB1 NPs at a concentration of 20  $\mu$ g mL<sup>-1</sup> for 6 h, and washed with PBS three times. For the control groups, cells were cultured only with pure cell medium. After laser light irradiation (808 nm), all cells were co-

incubated with Calcein AM and PI for 30 min, washed with PBS three times and the fluorescence microscope images were obtained. The excitation wavelength was 488 nm for Calcein AM and 561 nm for PI.

### **Animal experiments**

Female BALB/c mice (six-week-old) were obtained from Jilin University. All animal experiments were approved by the guidelines of the Committee on Animal Use and Care of Changchun Institute of Applied Chemistry, Chinese Academy of Sciences. The tumor-bearing models were established by inoculating subcutaneously murine 4T1 cancer cells (100  $\mu$ L,  $1 \times 10^6$  cells/mL in PBS) into the back site of each mouse.

### **In vivo phototherapy, photothermal imaging**

When the tumor volume reached about 100 mm<sup>3</sup>, the mice were randomly divided into 4 groups (n = 6). For the CB1 and “CB1 + laser” groups, the mice were injected with the CB1 NPs (200  $\mu$ g mL<sup>-1</sup>, 100  $\mu$ L) in PBS solution, whilst for the control groups (PBS and “PBS + laser”), PBS was injected. 10 h after administration, the tumors of the “PBS + laser” and “CB1 + laser” groups were irradiated for 10 min with laser light (808 nm, 0.8 W cm<sup>-2</sup>), whilst the mice in the PBS group and the CB1 group were not irradiated. Tumor volume and body weight of the mice were measured every 2 days continuously for 18 days. The tumor size was calculated as follows: volume = (tumor length)  $\times$  (tumor width)<sup>2</sup>/2. After the treatment, one mouse from each group was sacrificed for H & E and TUNEL staining of the tumors. In addition, major

organs were isolated and fixed in 4% formaldehyde solution, followed by histology analysis. The images of the tissue sections were recorded on a microscope.

For photothermal imaging, the mice were injected with the CB1 NPs ( $200 \mu\text{g mL}^{-1}$ ,  $100 \mu\text{L}$ ). The tumors were irradiated with laser light ( $808 \text{ nm}$ ,  $0.8 \text{ W cm}^{-2}$ ), the tumor temperature was captured by an IR camera.

### **In vivo biosafety evaluation**

Hematological parameters, including the amounts of white blood cell, lymphocyte, red blood cell, were obtained via standard blood examination. Liver function was investigated via reporting the amounts of albumin, aspartate aminotransferase and alanine aminotransferase. Kidney function was evaluated via measuring the blood urea nitrogen level.

### **In vivo NIR-II fluorescence imaging**

Nude mice were injected with 4T1 cells into the back site as the tumor model. Three mice were selected to perform the NIR-II fluorescence imaging. The mice were intravenously injected with the CB1 NPs ( $1 \text{ mg mL}^{-1}$ ,  $100 \mu\text{L}$ ) and the fluorescence microscopy images were captured at different time intervals. The dose of power density of laser for tumor imaging was  $0.063 \text{ W cm}^{-2}$ . After 48 h, the mice were sacrificed and fluorescence images of tumor, heart, liver, lung, kidney and spleen were recorded.

## Supporting Figures

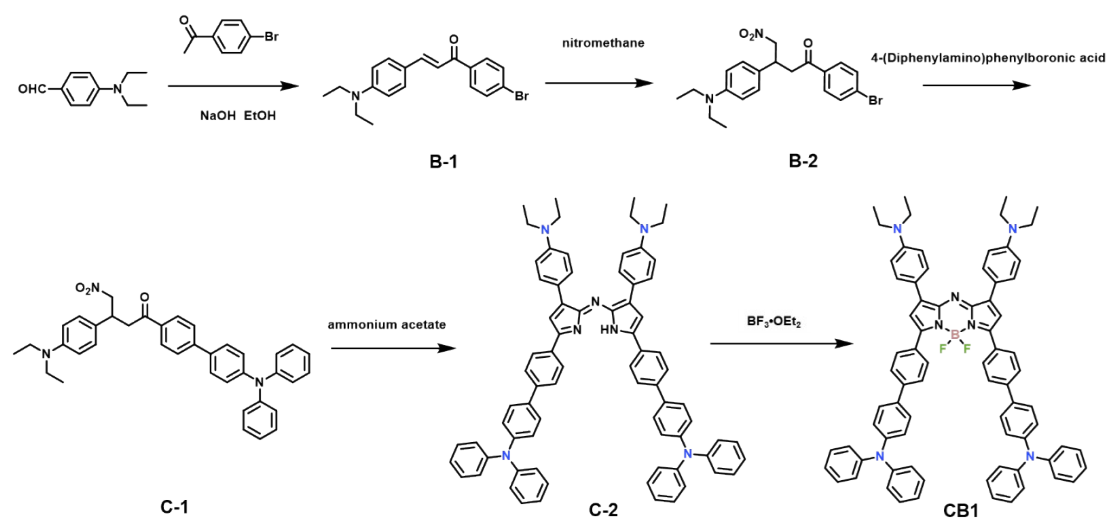


Figure S1. Synthetic route for CB1.

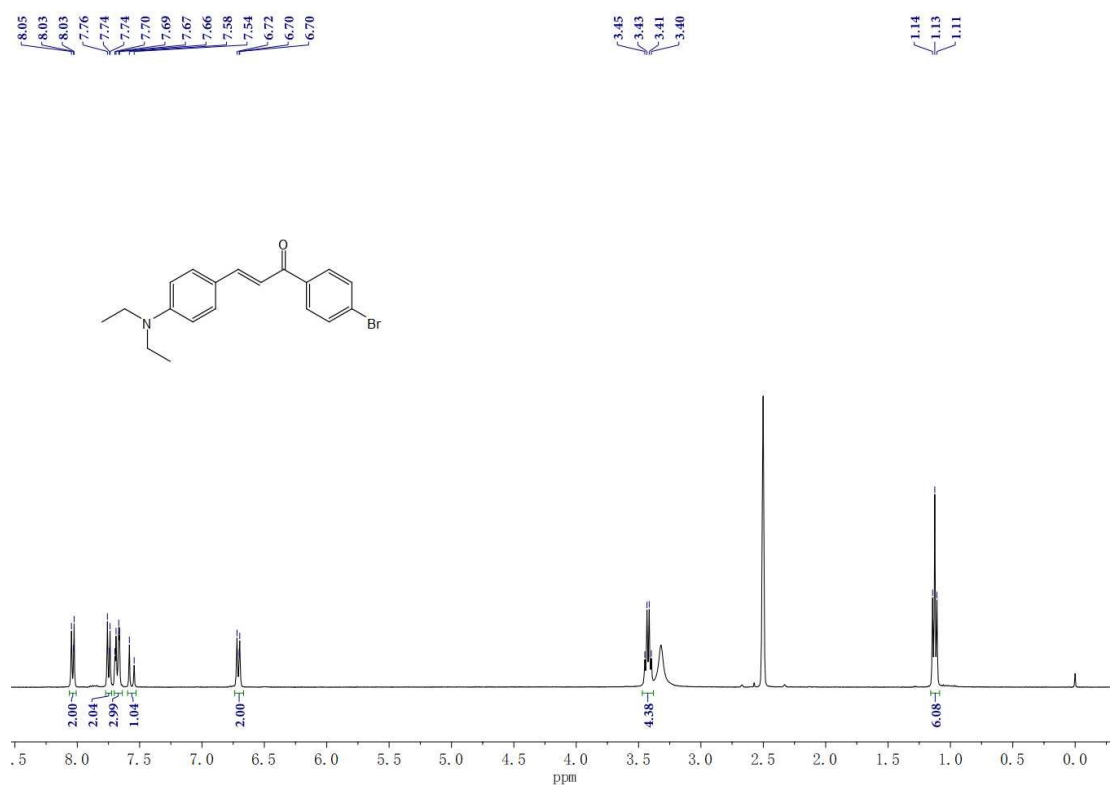
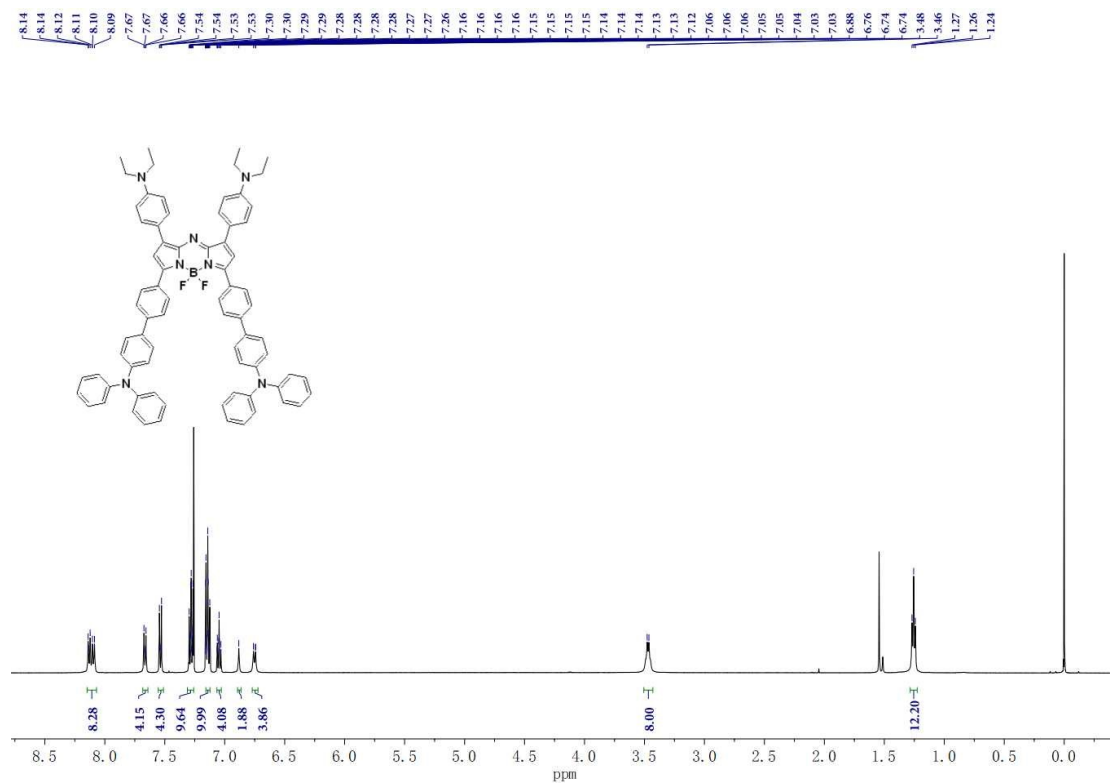
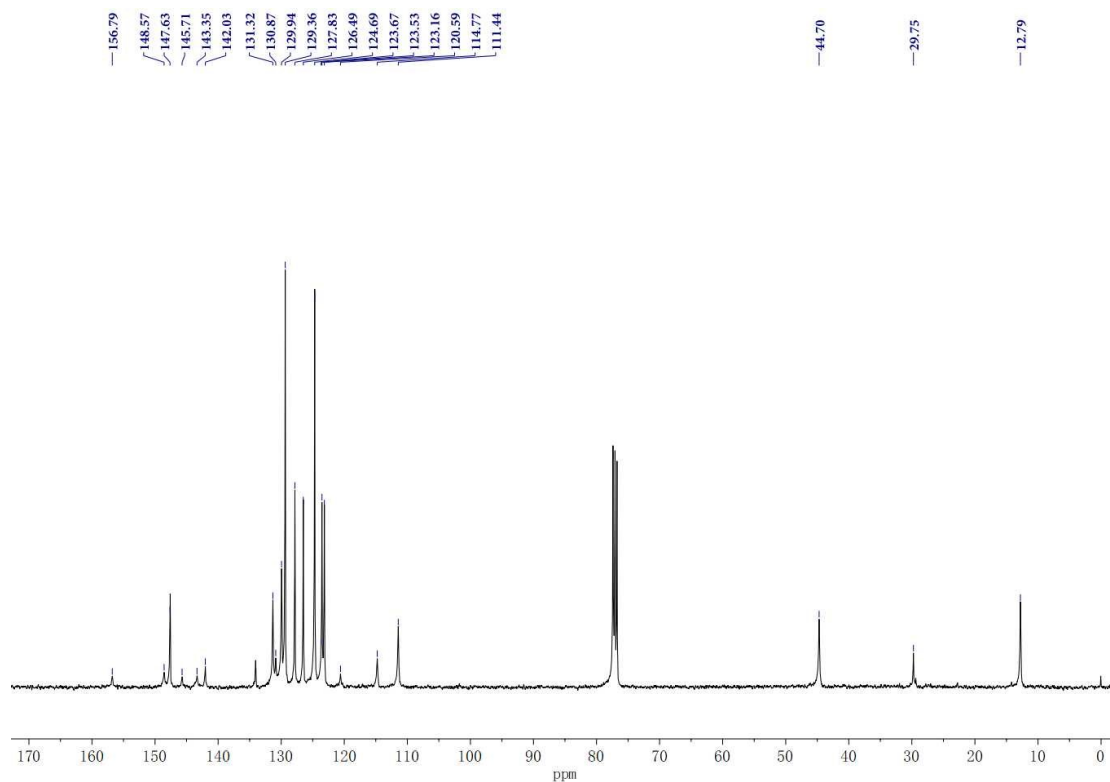


Figure S2.  $^1\text{H}$  NMR spectrum of **B-1** in  $\text{DMSO}-d_6$ .





**Figure S5.** <sup>1</sup>H NMR spectrum of CB1 in CDCl<sub>3</sub>.



**Figure S6.** <sup>13</sup>C NMR spectrum of CB1 in CDCl<sub>3</sub>.

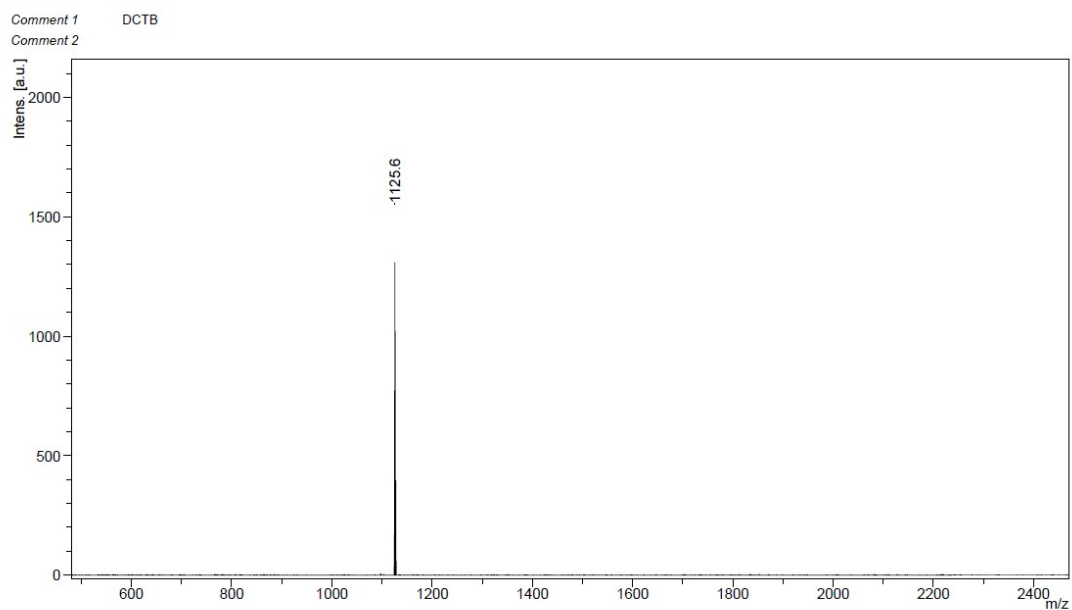


**Figure S7.** MALDI-TOF of CB1 in  $\text{CHCl}_3$ .

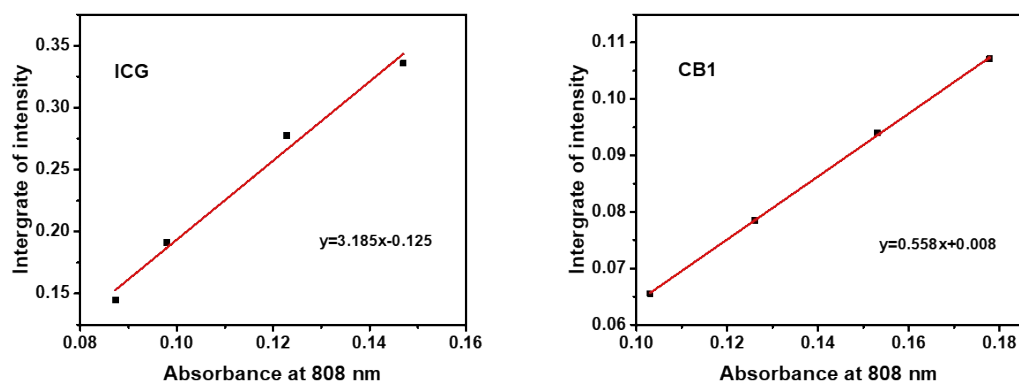


**Figure S8.** Fluorescence quantum yield measurement of CB1 in DMSO.

**Table S1.** Photophysical properties of several reported NIR-II luminogens.

Probe	$\lambda_{\text{em}}$ (nm)	Quantum yield (%)	Reference
IR1048	1048	0.4	S3
IR1061	1061	1.7	S3

<b>IR1026</b>	1026	0.5	S4
<b>TAB-2Br</b>	1002	0.088	S5
<b>NJ1030</b>	1030	0.2	S6
<b>NJ1060</b>	1060	1	S6
<b>IR 26</b>	1130	0.1	S7
<b>CB1</b>	1045	2.3	This work

Polymethine cyanine dyes usually exhibit small Stokes shift and are prone to photobleaching,<sup>S8-S9</sup> while CB1 possesses large Stokes shift of about 185 nm which is beneficial for reducing background noises, it also exhibits excellent photostability which is favorable for long-term in vivo bioimaging. Some BBTD-core NIR-II probes show excellent fluorescence quantum yield (for example, > 5%), however, the molar extinction coefficient is usually not very high ( $\epsilon_{\text{BBTD-cores}} \approx 10^3\text{-}10^4 \text{ M}^{-1} \text{ cm}^{-1}$ ).<sup>S10-S11</sup> CB1 possesses higher molar extinction coefficient ( $\epsilon \approx 4.8 \times 10^4 \text{ M}^{-1} \text{ cm}^{-1}$ ), the overall brightness ( $\epsilon_{\text{max}}\Phi_f$ ) and imaging performance are thus comparable. It should also be pointed out that CB1 shows low solubility and low quantum yield in aqueous solution. These drawbacks may be improved by fine tuning of the D-A-D structures.

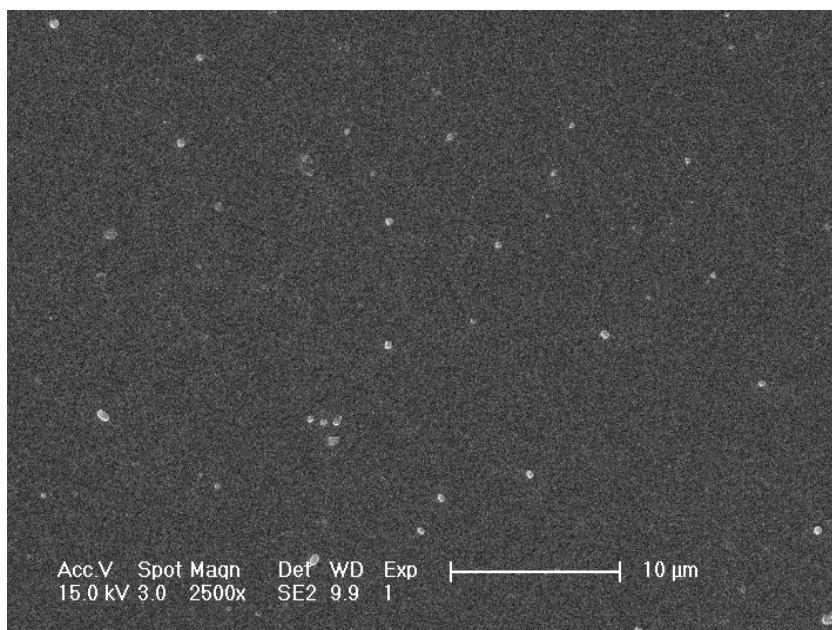


**Figure S9.** SEM image of the CB1 NPs.

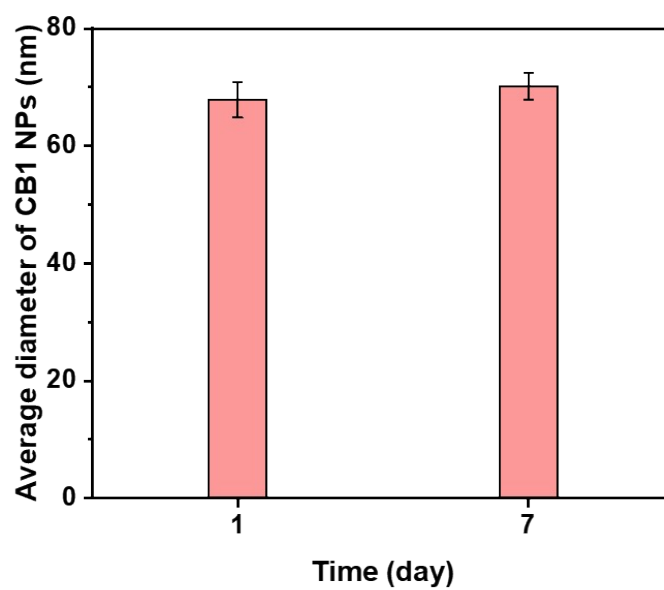


**Figure S10.** Stability of the CB1 NPs in PBS solution. NPs were dispersed in PBS for different periods of time and particle size was measured by DLS.

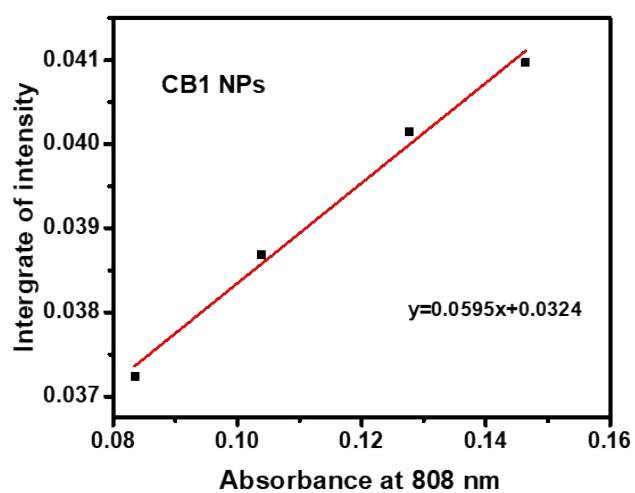


**Figure S11.** Fluorescence quantum yield measurement of the CB1 NPs in PBS solution.

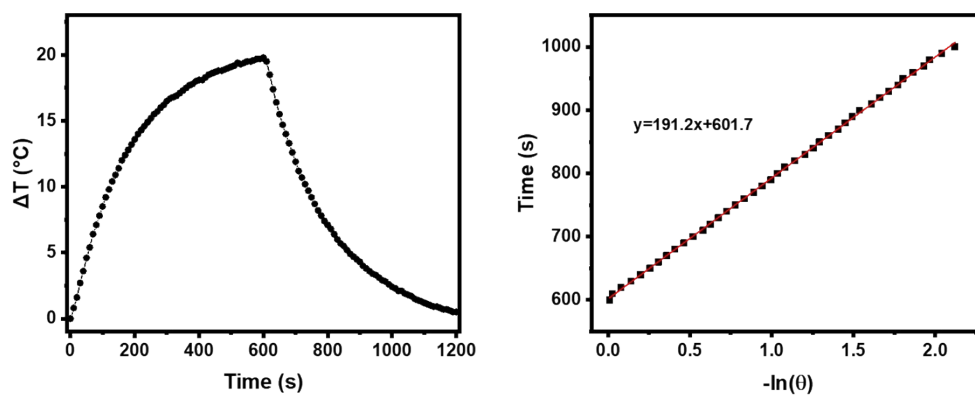


**Figure S12.** Temperature changes of the CB1 NPs assay solution under one on-off laser irradiation cycle, and the linear fitting of  $-\ln\theta$  with time. Conditions: 808 nm laser irradiation at  $1 \text{ W cm}^{-2}$ .

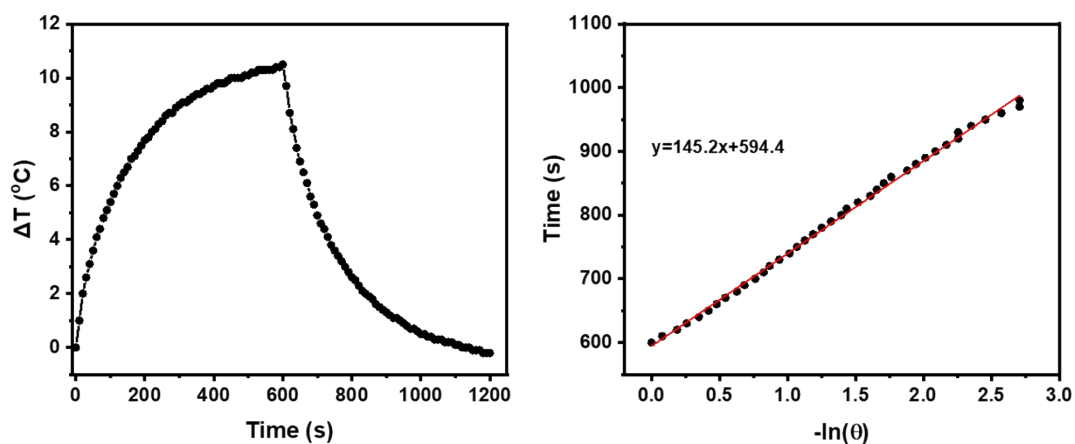


**Figure S13.** Temperature changes of the CB1 assay solution under one on-off laser irradiation cycle, and the linear fitting of  $-\ln\theta$  with time. Conditions: 808 nm laser irradiation at  $1 \text{ W cm}^{-2}$ . Photothermal conversion efficiency of CB1 ( $10 \mu\text{g mL}^{-1}$ ) in aqueous solution (1% DMSO in water) was tested to be 22.3%.

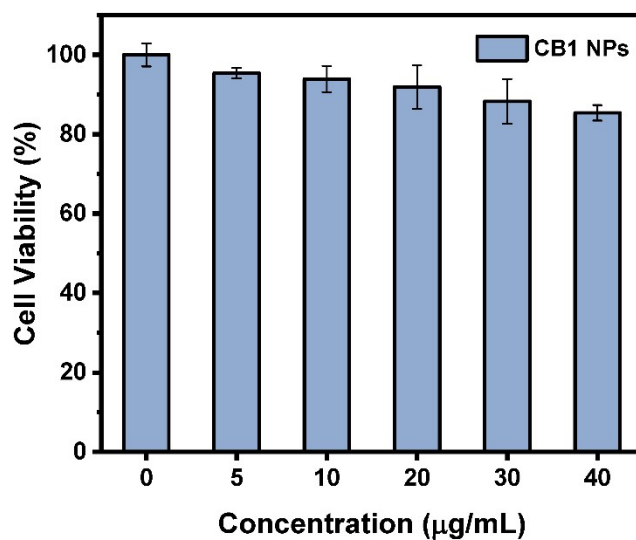


**Figure S14.** MTS assay of L929 cells in the presence of the CB1 NPs without laser irradiation.

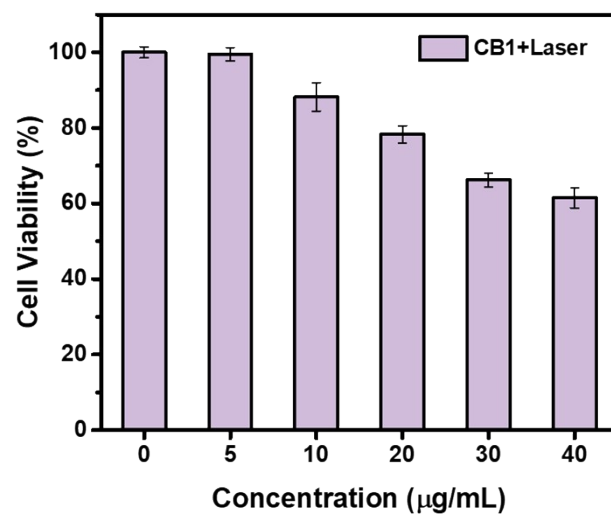


**Figure S15.** MTS assay of 4T1 cells in the presence of CB1 with laser irradiation.

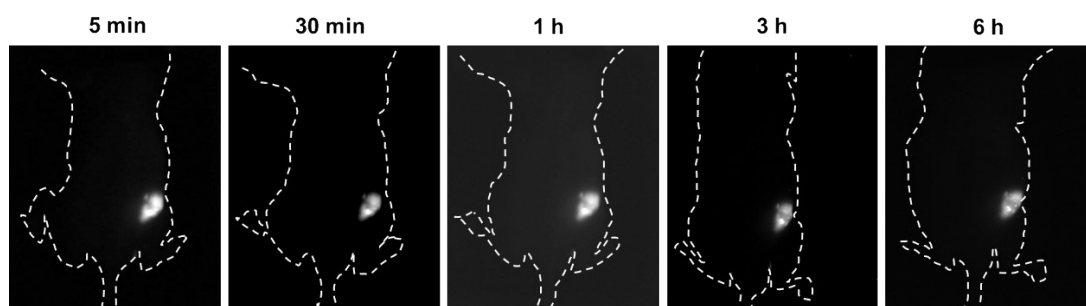


**Figure S16.** NIR-II fluorescence imaging of tumor on mice after intratumoral injection of the CB1 NPs for different periods of time.

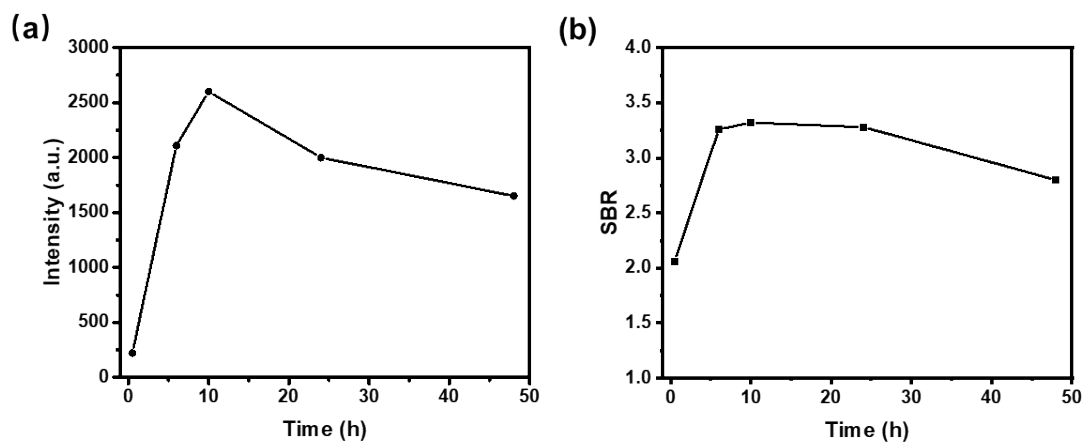


**Figure S17. (a)** Fluorescence intensity and **(b)** SBR changes at different time points at the tumor site after the injection of the CB1 NPs by the tail vein of the 4T1 tumor-bearing mice.

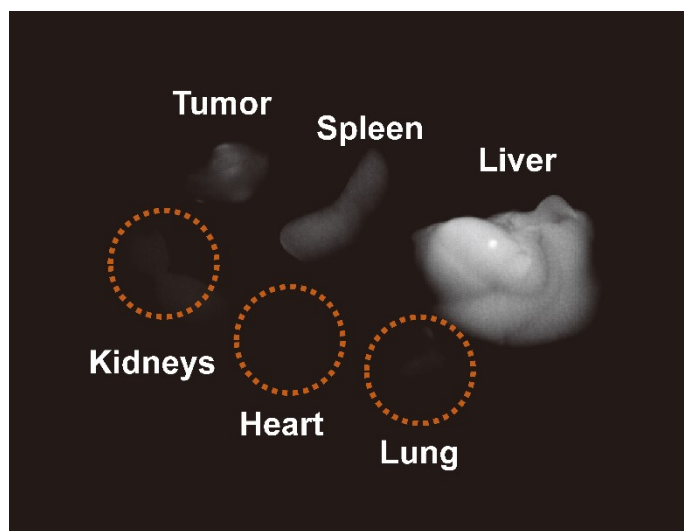


**Figure S18.** NIR-II fluorescence imaging of major organs and the tumor of the 4T1 tumor-bearing mouse after 48 h post-injection of the CB1 NPs.

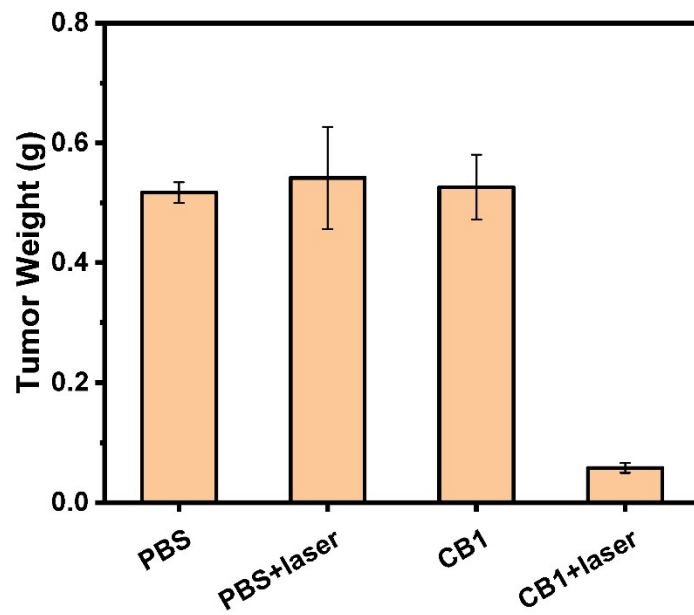


**Figure S19.** Tumor weight after various treatments.

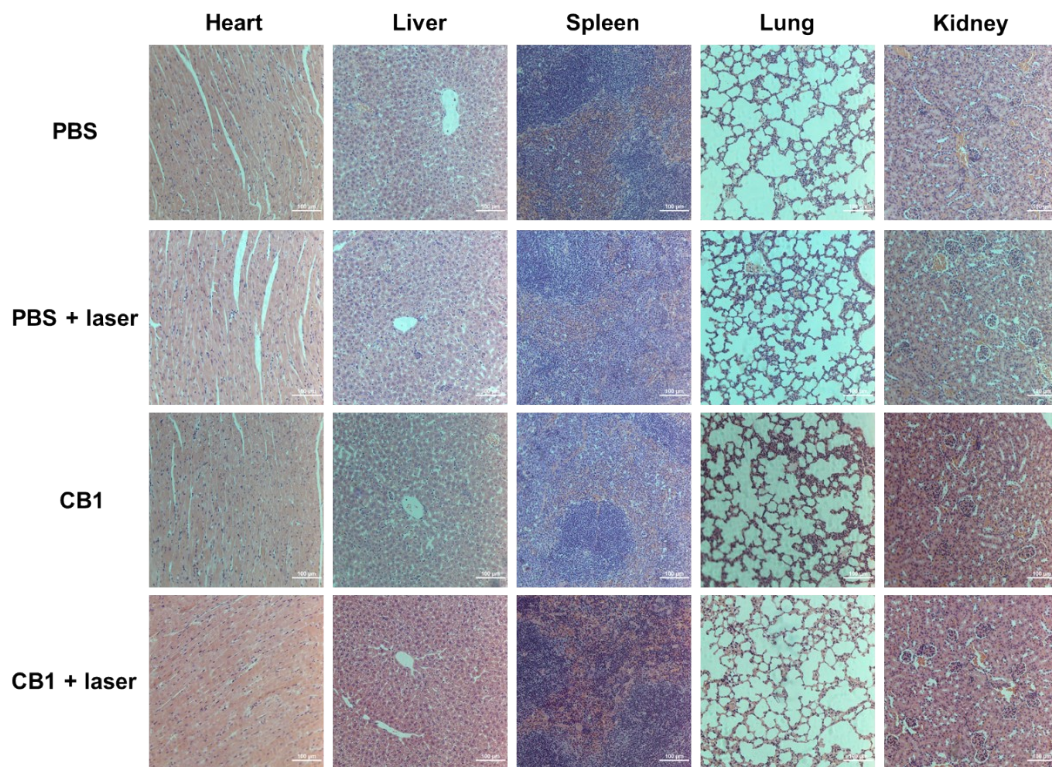


**Figure S20.** H & E staining of heart, liver, spleen, lung, and kidney of the mice under different treatments. Scale bar: 100 µm.

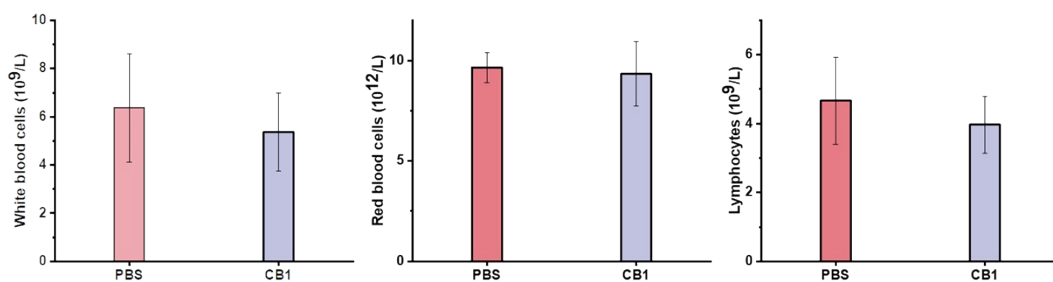


**Figure S21.** Changes in quantity of white blood cell, red blood cell, and lymphocyte in the blood of the mice injected with PBS or the CB1 NPs.

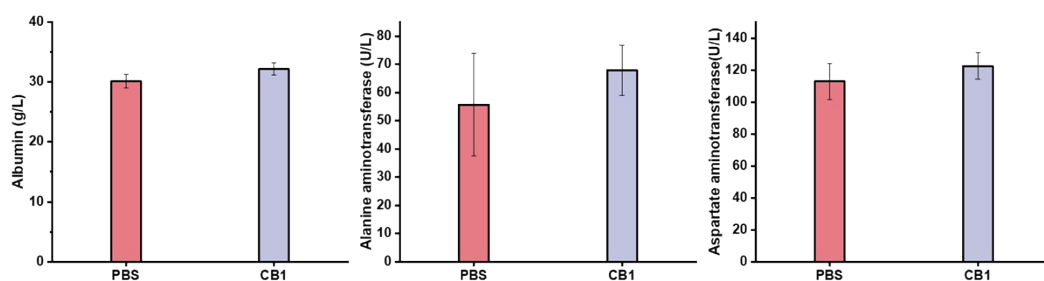


**Figure S22.** Changes in quantity of albumin, alanine aminotransferase, and aspartate aminotransferase of the mice injected with PBS or the CB1 NPs.

## References

- (S1) Zhou, X.; Zhang, K.; Yang, C.; Pei, Y.; Zhao, L.; Kang, X.; Li, Z.; Li, F.; Qin, Y.; Wu, L. Ultrabright and Highly Polarity-Sensitive NIR-I/NIR-II Fluorophores for the Tracking of Lipid Droplets and Staging of Fatty Liver Disease. *Adv. Funct. Mater.* **2022**, *32*, 2109929.
- (S2) Zou, J.; Li, L.; Zhu, J.; Li, X.; Yang, Z.; Huang, W.; Chen, X. Singlet Oxygen “Afterglow” Therapy with NIR-II Fluorescent Molecules. *Adv. Mater.* **2021**, *33*, 2103627.
- (S3) Proposito, P.; Casalboni, M.; De Matteis, F.; Glasbeek, M.; Quatela, A.; van Veldhoven, E.; Zhang, H. Femtosecond dynamics of IR molecules in hybrid materials. *J. Lumin.* **2001**, *94-95*, 641-644.

- (S4) Pizzoferrato, R.; Casalboni, M.; De Matteis, F.; Proposito, P. Optical investigation of infrared dyes in sol-gel films. *J. Lumin.* **2000**, *87-89*, 748-750.
- (S5) Tian, Y.; Zhou, H.; Cheng, Q.; Dang, H.; Qian, H.; Teng, C.; Xie, K.; Yan, L. Stable twisted conformation aza-BODIPY NIR-II fluorescent nanoparticles with ultra-large Stokes shift for imaging-guided phototherapy. *J. Mater. Chem. B* **2022**, *10*, 707-716.
- (S6) Bai, L.; Sun, P.; Liu, Y.; Zhang, H.; Hu, W.; Zhang, W.; Liu, Z.; Fan, Q.; Li, L.; Huang, W. Novel aza-BODIPY based small molecular NIR-II fluorophores for in vivo imaging. *Chem. Commun.* **2019**, *55*, 10920-10923.
- (S7) Hatami, S.; Würth, C.; Kaiser, M.; Leubner, S.; Gabriel, S.; Bahrig, L.; Lesnyak, V.; Pauli, J.; Gaponik, N.; Eychmüller, A.; Resch-Genger, U. Absolute photoluminescence quantum yields of IR26 and IR-emissive Cd<sub>1-x</sub>Hg<sub>x</sub>Te and PbS quantum dots-method-and material-inherent challenges. *Nanoscale* **2015**, *7*, 133-143.
- (S8) Li, B.; Lu L.; Zhao M., Lei, Z.; Zhang, F. An Efficient 1064 nm NIR-II Excitation Fluorescent Molecular Dye for Deep-Tissue High-Resolution Dynamic Bioimaging. *Angew. Chem., Int. Ed.* **2018**, *57*, 7483.
- (S9) Su, Y.; Yu, B.; Wang, S.; Cong, H.; Shen, Y. NIR-II bioimaging of small organic molecule. *Biomaterials*, **2021**, *271*, 120717.
- (S10) Yang, Q; Hu, Z.; Zhu, S.; Ma, R.; Ma, H.; Ma, Z.; Wan, H.; Zhu, T.; Jiang, Z.; Liu, W.; Jiao, L.; Sun, H.; Liang, Y.; Dai, H. Donor Engineering for NIR-II Molecular Fluorophores with Enhanced Fluorescent Performance. *J. Am. Chem. Soc.* **2018**, *140*, 1715-1724.
- (S11) Lei, Z.; Zhang, F. Molecular Engineering of NIR-II Fluorophores for Improved Biomedical Detection. *Angew. Chem. Int. Ed.* **2021**, *60*, 16294-16308.